In-Site Real-Time Photovoltaic *I–V* Curves and Maximum Power Point Estimator

José M. Blanes, F. Javier Toledo, Sergio Montero, and Ausiàs Garrigós, *Member, IEEE*

***Abstract*—This paper presents a practical implementation of a photovoltaic *I–V* curves and maximum power point estimation algorithm (IVMPPE). The IVMPPE estimates the *I–V* curve and sets the operation of the solar panels at a voltage that extracts the maximum available power without tracking. The operation is based on solving the parameters of the solar array equivalent electrical model, in real time, only with the measurements of six voltage and current coordinates near the operating point. Moreover, the strategy for selecting the measured points and the discard procedures for incorrect estimated curves are also detailed. To validate the IVMPPE, it has been tested under different operating conditions, and its accuracy has been compared with the classical perturb and observe (P&O) technique. The distinguishing feature of the IVMPPE is that complete *I–V* model is obtained, not only the MPP, enlarging the capabilities to other fields, e.g., real-time monitoring and prediction.**

***Index Terms*—Curve fitting, maximum power point tracker (MPPT), perturb and observe (P&O), photovoltaic (PV), renewable energy.**

I. Introduction

RENEWABLE energy sources are especially attractive for power generation due to their wide availability and their intrinsic clean energy nature. Among other renewable sources (as wind, biomass, geothermal, wave and tide, etc...), solar energy systems have been highly developed during the last three decades. Although being a very attractive and popular energy source, it still exhibits low light to electrical conversion efficiency [1], which directly impacts in its energy payback time.

In order to extract the maximum available power from photovoltaic (PV) modules a group of electronic circuits has been introduced during the last two decades: the maximum power point trackers (MPPT). The function of the MPPTs is to create the correct feedback signals in a power converter control loop, in such a way that PV generators are positioned at a voltage point that draws the maximum power available at any time.

Manuscript received May 23, 2012; revised June 6, 2012 and June 22, 2012; accepted June 26, 2012. Date of current version October 12, 2012. Recommended for publication by Associate Editor S. Valkealahti.

J. M. Blanes, S. Montero, and A. Garrigos are with the Department of Materials Science, Optical And Electronic Technology, University Miguel Hernandez of Elche, 03202 Elche, Spain (e-mail: jmblanes@umh.es; smontero@umh.es; augarsir@umh.es).

F. J. Toledo is with the Center of Operations Research, University Miguel Hernandez, 03202 Elche, Spain (e-mail: javier.toledo@umh.es).

Digital Object Identifier 10.1109/TPEL.2012.2206830

In addition, PV systems monitoring is another important issue regarding performance analysis, failure detection and maintenance costs and time reduction. In the literature, MPPT and monitoring are usually discussed as independent subjects.

A large number of MPPT techniques have been developed [2], currently most of them are digitally implemented because of the advances that modern microcontrollers and digital signal processors (DSP) provide in terms of flexibility and reusability. Such techniques are commonly known as digital maximum power point trackers (DMPPT) [3]. Some DMPPT examples reported in the literature are summarized as follows:

1) The perturb and observe (P&O) technique and its optimizations to reduce its oscillations around the MPP or to speed up its convergence under rapidly changing illumination conditions [4]–[7].
2) The incremental conductance method (INCOND) that compares the static and the incremental conductance to track the MPP. This method is well suited for rapid variations of atmospheric conditions [8], [9].
3) Root finding-based algorithms [3], [10]–[12] that treat the MPP location as a mathematical root finding problem. They search the point where the derivative of the power delivered with respect to the voltage is 0. These methods avoid oscillations once the MPP is found.
4) Chaotic search methods [13] apply the chaos theory to search the optimal value of the power extracted from the system. These methods have been applied for dealing with local maximum of PV systems under partially shadowing conditions.
5) Fuzzy logic controllers (FLC) [14] use fuzzy theory and usually track the MPP computing the slope and the slope change of the power-current characteristic of the PV system.

One common characteristic of all the techniques aforementioned is that they are kind of *"blind"* techniques. All of them search the MPP without getting out the full *I–V* curve of the system. Nowadays this aim could be tackled thanks to the microcontrollers and DSPs processing capabilities.

I–V curve estimation has been usually dealt in the literature as a different subject, basically for PV cells modeling purposes. Most of these techniques solve the electrical model of a solar cell [15], made of some discrete components, under controlled conditions of temperature and irradiance. Then, the model is extrapolated to other conditions, but the actual information of irradiance and temperature is required, increasing cost and complexity. In the literature, many different techniques have been developed to model the solar cells, some examples are as follows:

1) Curve fitting techniques [16] that rely on sweeping the whole *I–V* curve from open circuit to short circuit.
2) Analytical five-point method [17]. This method only need the measurement of five points to extract the *I–V* curve, but these points are: the short-circuit point, the open circuit point, the MPP, as well as the slopes of the curve in the short-circuit and open-circuit points.
3) Particle swarm optimization methods [18], [19]. These methods are initiated with a population of random solutions. Then, an iterative function optimizes such solutions and creates a family of *I–V* curves. Finally, one curve is chosen as the right solution by comparing the model and the provided manufacturer data.

None of these methods can be used in real time, in-site PV monitoring since measuring open circuit and short circuits points is in many cases impossible, and in other ones, causes an unacceptable power loss.

In [20], it is presented a curve fitting method that only needs the measurement of four working points near the MPP to obtain the *I–V* curve in real time, but the fitting accuracy over the whole curve is generally poor. In [21], this technique has been improved using six pairs of voltage and current points. In both cases, the *I–V* curve is estimated under any working conditions, besides, required points do not swing excessively from the actual operating point and, consequently, power losses during estimation phase are minimal. Once the *I–V* curve is computed, MPP can be easily calculated and the system achieves MPP without oscillations. Applying this technique, MPP and complete *I–V* curve information is available in real time without any extra information, e.g., manufacturer data, irradiance, or temperature sensors.

In [21] the mathematical development of the proposed estimation technique and a method to compute the MPP can be found, but all the tests were performed in steady-state conditions. In this paper, a real-time implementation of such technique is described. It is also detailed the optimal distribution of the sensed points and how to discard incorrect estimated curves. To validate the *I–V* curves and maximum power point estimation (IVMPPE) concept, it has been tested under different working conditions, and the accuracy has been compared with the classical P&O technique.

This paper is organized in five sections. In Section II, the IVMPPE method is presented. In Section III, an optimal selection procedure of the measured points is explained. In Section IV, experimental results are presented. Section V shows a passive implementation of the IVMPPE technique, only used for monitoring purposes. Section VI summarizes and concludes this paper.

II. *I–V* Curve and MPP Estimation Algorithm

The IVMPPE algorithm solves the single-diode, four-parameter model with the measurement of six pairs of voltage and current points near the actual operating point. A complete description of the algorithm can be found in [17], but for the sake of clarity, a description is presented shortly.

The four-parameter model equation starts with the electrical model of an individual solar cell, where the shunt resistance has been neglected [8]. A PV module or solar array is then obtained by an arrangement of series and parallel cells [22] and results in (1)

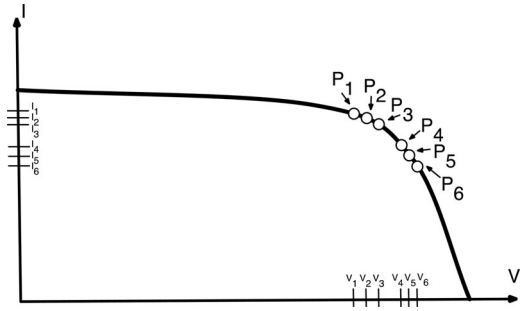

Fig. 1. Points used by the IVMPPE algorithm.

$$I = n_p I_{\rm ph} - n_p I_{\rm sat}(e^{(V+IR_s n_s/n_p)q/(n_s kT)} - 1) \quad (1)$$

where I is the PV array current, V is the PV array voltage, $I_{\rm ph}$ is the photocurrent, $I_{\rm sat}$ is the diode saturation current, q is the electronic charge, k is Boltzman's constant, T is the temperature, n_p is the number of PV cells in parallel, and n_s is the number of PV cells in series. Using the notation detailed in (2)

$$A = n_p I_{\rm ph},\ B = n_p I_{\rm sat},\ C = e^{q/(n_s kT)},\quad D = e^{R_s q/(n_p kT)}). \quad (2)$$

Equation (1) can be written as follows:

$$I = A - B(C^V D^I - 1) \quad (3)$$

$$V(I) = \frac{\ln(A + B - I) - \ln(B) - I\ln(D)}{\ln(C)}. \quad (4)$$

If $K = A + B$, the first and the second derivatives become the following equation, respectively:

$$V'(I) = \frac{1}{\ln(C)}\left(\frac{-1}{K - I} - \ln(D)\right) \quad (5)$$

$$V''(I) = \frac{1}{\ln(C)}\left(\frac{-1}{(K - I)^2}\right). \quad (6)$$

The estimation algorithm solves these four parameters (*A*, *B*, *C*, and *D*) without the need of any more information than the voltage and current of two arbitrary points of the PV installation, and the first and second derivatives of these points. As this information cannot be directly extracted from a PV installation, the first and the second derivatives are approximated by means of two blocks of three pairs of current–voltage coordinates near the working point ($(V_1, I_1), (V_2, I_2), (V_3, I_3)$ and $(V_4, I_4), (V_5, I_5), (V_6, I_6)$) (see Fig. 1).

The required condition for these points is that they must be distributed in two individual blocks of three coordinates each. In each group, the points must be close to each other. Satisfying such condition, the derivatives become as follows:

$$I_{12} = \frac{I_1 + I_2}{2},\ I_{23} = \frac{I_2 + I_3}{2},\ I_{45} = \frac{I_4 + I_5}{2},\ I_{56} = \frac{I_5 + I_6}{2} \quad (7)$$

$$I_{23} = \frac{I_1 + I_2 + I_3}{3},\quad I_{456} = \frac{I_4 + I_5 + I_6}{3} \quad (8)$$

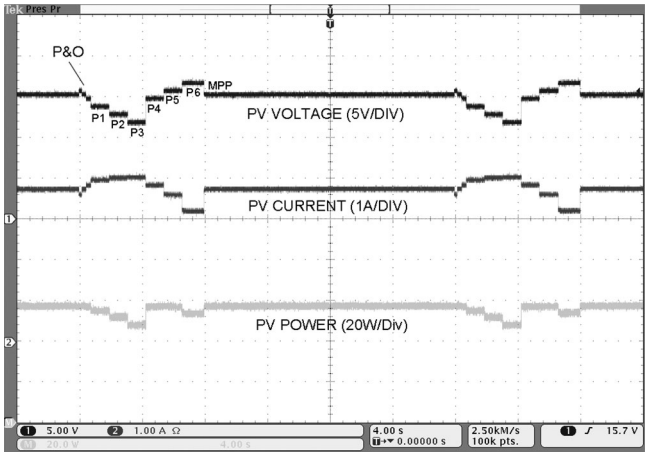

Fig. 2. IVMPPE algorithm oscilloscope screenshot.

$$V'_{12} = \frac{V_2 - V_1}{I_2 - I_1}, \quad V'_{23} = \frac{V_3 - V_2}{I_3 - I_2}, \quad V'_{45} = \frac{V_5 - V_4}{I_5 - I_4},$$
$$V'_{56} = \frac{V_6 - V_5}{I_6 - I_5} \tag{9}$$

$$V''_{123} \frac{V'_{32} - V'_{12}}{I_{23} - I_{12}}, \quad V''_{456} = \frac{V'_{56} - V'_{45}}{I_{56} - I_{45}}. \tag{10}$$

Parameter K comes from the quotient $\mathrm{V}''_{123}/\mathrm{V}''_{456}$

$$K = \frac{I_{456} - I_{123}\sqrt{V''_{123}/V''_{456}}}{1 - \sqrt{V''_{123}/V''_{456}}}. \tag{11}$$

And finally, A, B, C, and D are given as follows:

$$C = e^{\left(\frac{-1}{V''_{123}(k - I_{123})^2}\right)}, \quad D = e^{\left(\frac{-V'_{56}\ln(C)}{k - I_{56}}\right)},$$
$$B = \frac{K - I_6}{C^{V_6} D^{I_6}}, \quad A = K - \frac{K - I_6}{C^{V_6} D^{I_6}}. \tag{12}$$

From the previous analysis, it is concluded that the *I–V* curve can be estimated without any extra information as temperature, irradiance, or PV configuration details. Once the *I–V* curve has been estimated, the calculation of the MPP is a trivial problem that can be solved with any numerical method, two examples are the Newton–Raphson method used in [16] and the fix point method described in [17].

III. Optimal Selection of Sensed Coordinates

For the practical implementation, some issues must be taken into account in order to guarantee consistent *I–V* curve estimation and MPP computation. For instance, the algorithm could fail due to sensing errors, digital quantifications or sudden atmospheric changes during data acquisition. In this section, the conditions that must fulfil the sensed points and the calculated parameters are listed. In practice, these conditions are very useful, if the algorithm detects that any of these condition is not accomplished, it is automatically aborted, the curve discarded and the estimation restarted.

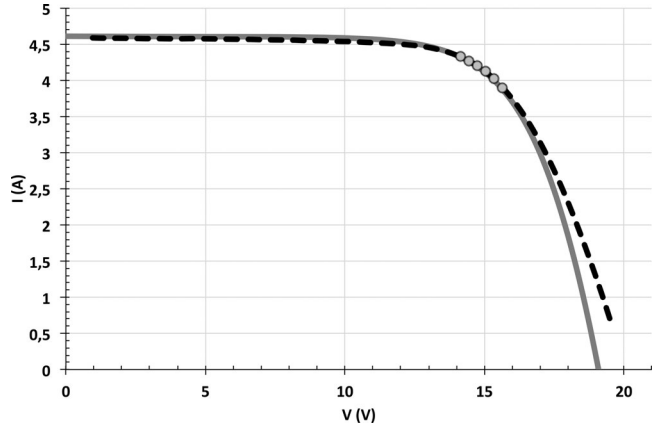

Fig. 3. *I–V* curve estimation with 2% of V_{MPP} voltage steps. *Solid Line*: real curve. *Dashed Line*: estimated curve. *Dots*: points used for the estimation.

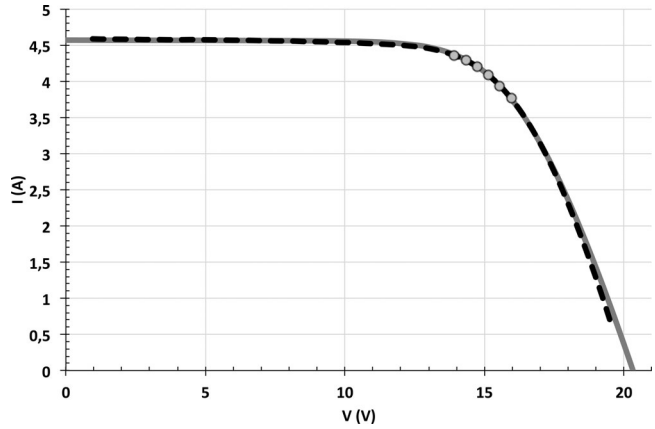

Fig. 4. *I–V* curve estimation with 2.5% of V_{MPP} voltage steps. *Solid Line*: real curve. *Dashed Line*: estimated curve. *Dots*: points used for the estimation.

Due to the *I–V* characteristic of a PV array, the conditions that must always fulfil the sensed points are

$$I_1 > I_2 > I_3 > I_4 > I_5 > I_6 \tag{13}$$
$$V_1 < V_2 < V_3 < V_4 < V_5 < V_6 \tag{14}$$
$$V'_{12} < V'_{23} < V'_{45} < V'_{56} \tag{15}$$
$$V''_{123} < V''_{456}. \tag{16}$$

If the measured points meet conditions (13)–(16), then the algorithm can be executed and the parameters A, B, C, and D computed. Otherwise, the acquiring process is repeated until valid points are obtained.

Moreover, the estimated curve is valid if and only if the following conditions are fulfilled:

$$I_{\mathrm{ph}} > 0 \Rightarrow A = n_p I_{\mathrm{ph}} > 0 \tag{17}$$
$$I_{\mathrm{sat}} > 0 \Rightarrow B = n_p I_{\mathrm{sat}} > 0 \tag{18}$$
$$\frac{q}{n_s kT} > 0 \Rightarrow C = e^{q/(n_s kT)} > 1 \tag{19}$$
$$R_s > 0 \Rightarrow \frac{R_s q}{n_p kT} > 0 \Rightarrow D = e^{R_s q/(n_p kT)} > 1. \tag{20}$$

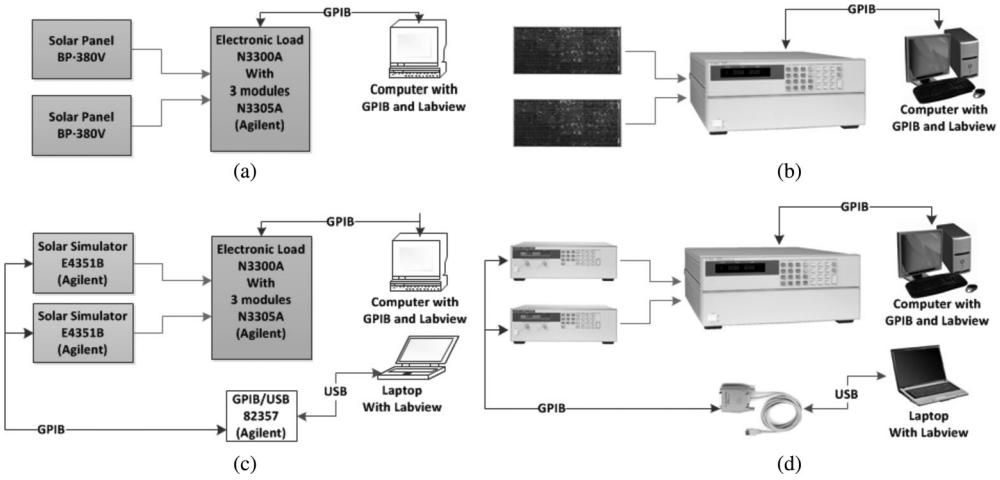

Fig. 5. Laboratory setup. (a) Schematic Diagram 1. (b) Connection Diagram 1. (c) Schematic Diagram 2. (d) Connection Diagram 2.

The location of the measured pairs is also important to perform accurate estimations. It is verified [20] that the optimal distribution places the first block (P1, P2, and P3) below the MPP and the second block (P4, P5, and P6) above it. The estimation and the P&O techniques have been mixed to achieve such distribution. P&O is used to find out the MPP and this point becomes P4 in the estimation algorithm. The rest of points are acquired using constant voltage steps. The voltage step value is a predefined percentage of the nominal MPP. The reason why MPP becomes P4 is because the slope of the P–V curve above the MPP is larger than below it, so power losses are minimized if only two points are measured in the right part (above MPP) of the curve.

The oscilloscope waveform, depicted in Fig. 2, shows the IVMPPE algorithm operation. P and O applies first and the MPP is found, then the first block (P1, P2, and P3) and second block (P4, P5, and P6) are acquired. Finally, the PV source voltage is set to the new MPP and remains unchanged until a current variation is detected or a preprogrammed timeout is raised.

Voltage step selection is a tradeoff between estimation accuracy, power losses during estimation process, and power electronics compatibility, i.e., allowed input voltage range in a practical converter. A minimum voltage step value of 2.5% of the MPP voltage has been found out by experimental tests. Figs. 3 and 4 illustrate the impact of voltage step selection. Fig. 3 shows estimated and real curves using voltage steps of 2% of the MPP voltage, it is clearly observed that estimated curve diverges from actual curve above the MPP. Fig. 4, however, shows high confidence level using a voltage step of 2.5% of the MPP voltage.

IV. Experimental Setup and Results

In order to evaluate the performance of the estimation algorithm as MPP tracker, both P&O and IVMPPE algorithms are implemented and compared under the same working conditions. The laboratory setup [see Fig. 5(a) and (b)] includes: two solar panels BP-380 from BP SOLAR, two electronic load modules (N3305 from Agilent) working at constant voltage mode and a computer that sets the load voltages. Both algorithms have been programmed in Labview and work in parallel. Moreover, each time the IVMPPE estimates a new curve this is saved in the computer memory and the MPP voltage is computed using the fix point method. No external voltage or current sensors are needed because the electronic load, via GPIB commands, provides voltage and current measurements.

TABLE I
Test 1 Characteristics

Parameter	*Value*
Date	3 November 2011
Start Hour	9:45
End Hour	16:31
P&O voltage steps	0.2V
IVMPPE MPP Voltage percentage used to acquire points.	2.5 %
IVMPPE Time-Out to recalculate	60 seg
IVMPPE current change percentage to recalculate	5 %
P&O Mean Power	53.04 W
IVMPPE Algorithm Mean Power	52.97 W

The first test was carried out during a full cloudless day and the main parameters are summarized in Table I.

Fig. 6 depicts the power extracted from the two solar modules with both the algorithms. The IVMPPE curve exhibits a small power drop each time the system acquires the six points, but the extracted power (see referred to the mean power in Table I) is almost the same in both methods because IVMPPE does not oscillate around the MPP. Figs. 7 and 8 show some of the curves estimated during this test.

Two solar array simulators (E4351B from Agilent) replace PV modules during the second test. Since the power delivered by the simulators is exactly the same, an accurate comparison of the power extracted by the two algorithms in steady-state conditions is possible. The main characteristics of the second test are summarized in Table II, whereas setup is shown in Fig. 5(c) and (d).

As was expected, the P&O accuracy is slightly higher than the IVMPPE. This is due to the fact that there are some power losses associated with the acquisition process; however, in terms of

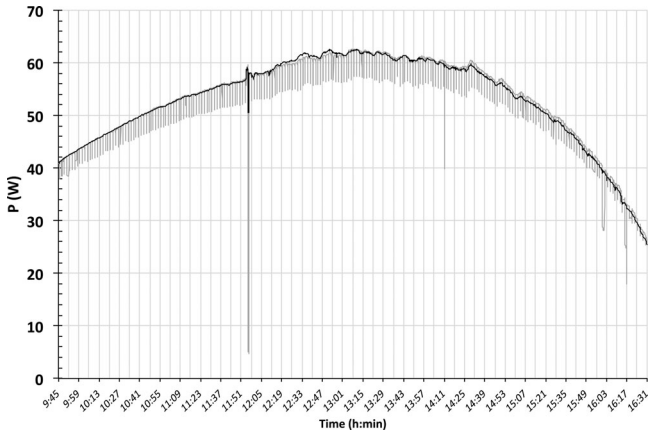

Fig. 6. Extracted power during test 1. *Gray Line*—IVMPPE algorithm *Black Line*—P and O algorithm.

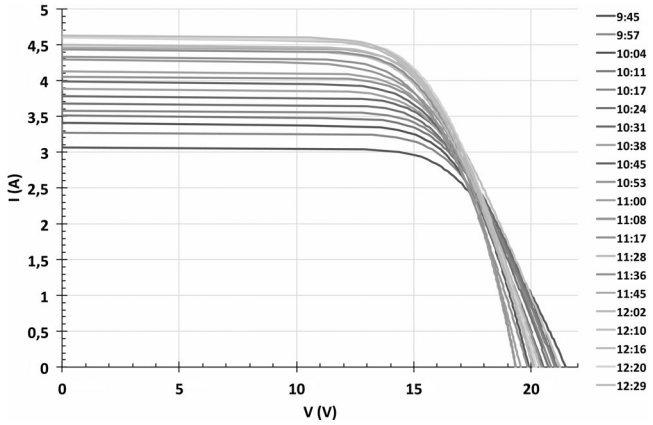

Fig. 7. Estimated curves during test 1 from 09:45 to 12:29.

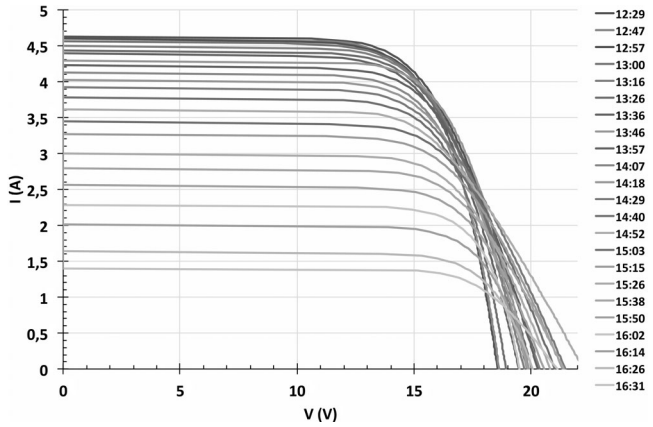

Fig. 8. Estimated curves during test 1 from 12:29 to 16:31.

average power, IVMPPE takes advantage of being a non oscillating method and eventually the power extraction is balanced.

In order to test the IVMPPE under rapidly changing conditions, a third test was carried out with the two algorithms running in parallel during 45 min in a cloudy day. Table III includes the main parameters and in Fig. 9 is presented the evolution of the power extracted during the test.

TABLE II
TEST 2 CHARACTERISTICS

Parameter	***Value***
Solar Array Simulators Programmed Curve	I_{SC}=3.7A, I_{MPP}=3.3A, V_{MPP}=14V, V_{OC}=20V
Test Duration	1 hour
P&O voltage steps	0.2V
IVMPPE MPP Voltage percentage used to acquire points.	2.5%
IVMPPE Time-Out to recalculate	60 seg
IVMPPE current change percentage to recalculate	5%
Solar Simulators MPP Power	46.2W
P&O Mean Power	45.92W
IVMPPE Algorithm Mean Power	45.70W
P&O Accuracy	99.39%
IVMPPE Accuracy	98.92%

TABLE III
TEST 3 CHARACTERISTICS

Parameter	***Value***
Date	10 November 2011
Start Hour	14:26
End Hour	15:10
P&O voltage steps	0.2V
IVMPPE MPP Voltage percentage used to acquire points.	2.5%
IVMPPE Time-Out to recalculate	60 seg
IVMPPE current change percentage to recalculate	5 %
P&O Mean Power	30.52 W
IVMPPE Algorithm Mean Power	30.41 W

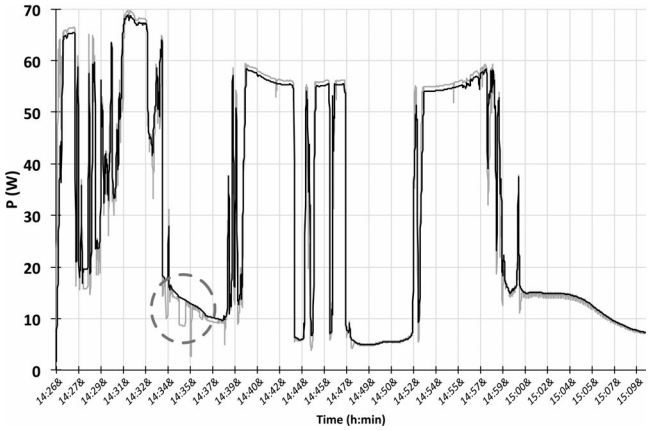

Fig. 9. Extracted power during test 3. *Gray Line*—IVMPPE algorithm, *Black Line*—P and O algorithm.

These results demonstrate the high-end performance of the IVMPPE at any working conditions. The power extracted is very similar to the P&O algorithm even under rapidly change conditions, where many curves points have been discarded during the estimation process. In Fig. 9 the only MPP estimation error is marked with a circle. In this case, the algorithm estimated a wrong *I–V* curve, and then a wrong MPP voltage was set. This error was not detected because the estimated curve was a valid PV curve and the algorithm did not discard it. Nevertheless, at

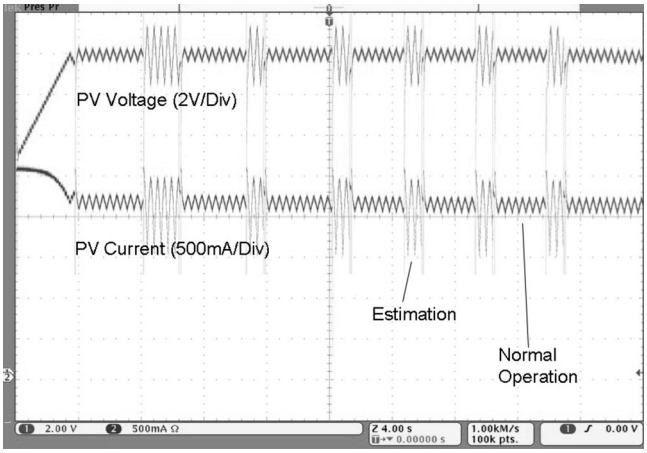

Fig. 10. Estimation algorithm working in passive mode.

the next iteration of the algorithm, the estimation was accurate and the correct MPP calculated again.

V. *I–V* Passive Mode Curve Estimation

This estimation method is also suitable for monitoring purposes only, without MPPT control in any actual PV MPPT power converter. For instance, the ripple of an analog MPPT can be temporarily increased to acquire points and then go back to nominal MPPT mode. Fig. 10 shows an oscilloscope screenshot where this concept is applied, an analog P&O method operates a PV system at the MPP and the MPPT ripple increases for estimation.

VI. Conclusion

This paper describes and implements an algorithm for *I–V* curve estimation. Practical applications for this method are MPP tracking but it is also valid for control or monitoring purposes. Theoretical developments are validated by an experimental setup and compared with the P&O technique under different working conditions. Experimental results show that the estimation algorithm provides accurate tracking in any working conditions. This accuracy is slightly lower than the one achieved with the P&O technique, but real-time information of the PV source is obtained.

References

[1] G. Acciari, D. Graci, and A. LaScala, "Higher PV module efficiency by a novel CBS bypass," *IEEE Trans. Power Electron*., vol. 26, no. 5, pp. 1333–1336, May 2011.

[2] T. Esram and P. Chapman, "Comparison of photovoltaic array maximum power point tracking techniques," *IEEE Trans. Energy Convers*., vol. 22, no. 2, pp. 439–449, Jun. 2007.

[3] C. Seunghyun and A. Kwasinski, "Analysis of classical root-finding methods applied to digital maximum power point tracking for sustainable photovoltaic energy generation," *IEEE Trans. Power Electron*., vol. 26, no. 12, pp. 3730–3743, Dec. 2011.

[4] C. Huang-Je, L. Yu-Kang, Y. Chun-Jen, and C. Shih-Jen, "Design and implementation of a photovoltaic high-intensity-discharge street lighting system," *IEEE Trans. Power Electron*., vol. 26, no. 12, pp. 3464–3471, Dec. 2011.

[5] N. Femia, G. Petrone, G. Spagnuolo, and M. Vitelli, "Optimization of perturb and observe maximum power point tracking method," *IEEE Trans. Power Electron*., vol. 20, no. 4, pp. 963–973, Jul. 2005.

[6] L. Whei-Min, H. Chih-Ming, and C. Chiung-Hsing, "Neural-network-based MPPT Control of a stand-alone hybrid power generation system," *IEEE Trans. Power Electron*., vol. 26, no. 12, pp. 3571–3581, Dec. 2011.

[7] A. K. Abdelsalam, A. M. Massoud, S. Ahmed, and P. N. Enjeti, "High-performance adaptive perturb and observe MPPT technique for photovoltaic-based microgrids," *IEEE Trans. Power Electron*., vol. 26, no. 4, pp. 1010–1021, Apr. 2011.

[8] K. H. Hussein, I. Muta, T. Hoshino, and M. Osakada, "Maximum photovoltaic power tracking: An algorithm for rapidly changing atmospheric conditions," *IEE Proc. Inst. Elect. Eng*., vol. 142, no. 1, pp. 59–64, Jan. 1995.

[9] Z. Longlong, W. G. Hurley, and W. H. Wölfle, "A new approach to achieve maximum power point tracking for PV system with a variable inductor," *IEEE Trans. Power Electron*., vol. 26, no. 4, pp. 1031–1037, Apr. 2011.

[10] F. Luo, P. Xu, Y. Kang, and S. Duan, "A variable step maximum power point tracking method using differential equation solution," in *Proc. 2nd IEEE Conf. Ind. Electron. Appl*, May 2007, pp. 2259–2263.

[11] W. Peng, H. Zhu, W. Shen, F. H. Choo, P. C. Loh, and K. K. Tan, "A novel approach of maximizing energy harvesting in photovoltaic systems based on bisection search theorem," in *Proc. IEEE Appl. Power Electron. Conf. Exp*., Feb. 2010, pp. 2143–2148.

[12] S. Chun and A. Kwasinski, "Modified regula falsi optimization method approach to digital maximum powerpoint tracking for photovoltaic application," in *Proc. IEEE Appl. Power Electron. Conf. Exp*., Mar. 2011, pp. 6–10.

[13] Z. Lin, C. Yan, G. Ke, and J. Fangcheng, "New approach for MPPT control of photovoltaic system with mutative-scale dual-carrier chaotic search," *IEEE Trans. Power Electron*., vol. 26, no. 4, pp. 1038–1048, Apr. 2011.

[14] B. N Alajmi, K. H. Ahmed, S. J. Finney, and B. W. Willians, "Fuzzy-logic-control approach of a modified hill-climbing method for maximum power point in microgrid standalone photovoltaic system," *IEEE Trans. Power Electron*., vol. 26, no. 4, pp. 1022–1029, Apr. 2011.

[15] J. Leppäaho and T. Suntio, "Dynamic characteristics of current-fed super-buck converter," *IEEE Trans. Power Electron*., vol. 26, no. 1, pp. 200–209, Jan. 2011.

[16] M. Haouari-Merbah, M. Belhamel, I. Tobias, and J. Ruiz, "Extraction and analysis of solar cell parameters from the illuminated current–voltage curve," *Solar Energy Mater. Solar Cells*, vol. 87, pp. 225–233, May 2005.

[17] J. C. Wang, Y. L. Su, J. C. Shieh, and J. A. Jiang, "High-accuracy maximum power point estimation for photovoltaic arrays," *Solar Energy Mater. Solar Cells*, vol. 95, pp. 843–851, Mar. 2011.

[18] K. Ishaque, Z. Salam, M. Amjad, and S. Mekhilef, "An improved particle swarm optimization (PSO)-based MPPT for PV with reduced steady-state oscillation," *IEEE Trans. Power Electron*., vol. 27, no. 8, pp. 3627–3638, Aug. 2012.

[19] J. J. Soon and K. S. Low, "Photovoltaic model identification using particle swarm optimization with inverse barrier constraint," *IEEE Trans. Power Electron*., vol. 27, no. 9, pp. 3975–3983, Sep. 2012.

[20] A. Garrigós, J. M. Blanes, J. A. Carrasco, and J. B. Ejea, "Real time estimation of photovoltaic modules characteristics and its application to maximum power point operation," *Renew. Energy*, vol. 32, pp. 1059–1076, May 2007.

[21] F. J. Toledo, J. M Blanes, A. Garrigos, and J. A. Martínez, "Analytical resolution of the electrical four-parameters model of a photovoltaic module using small perturbation around the operating point," *Renew. Energy*, vol. 43, pp. 83–89, Jul. 2012.

[22] J. Young-Hyok, J. Doo-Yong, K. Jun-Gu, K. Jae-Hyung, L. Tae-Won, and W. Chung-Yuen, "A real maximum power point tracking method for mismatching compensation in PV array under partially shaded conditions," *IEEE Trans. Power Electron*., vol. 26, no. 4, pp. 1001–1009, Apr. 2011.

José M. Blanes was born in Elche, Spain, in 1974. He received the M.Sc. degree on telecommunication engineering from the Universidad Politécnica de Valencia, Valencia, Spain, in 1998, and the Ph.D. degree on industrial technologies from the University Miguel Hernández de Elche (UMH), Elche, Spain, in 2011.

He is currently an Associate Professor in the Department of Materials Science, Optics and Electronics Technology, UMH. His main research interests include space power systems and industrial electronics.

F. Javier Toledo was born in Almoines, Valencia, Spain, in 1973. He received the M.Sc. degree in mathematics from the Universitat de València, Valencia, Spain, in 1997.

He is currently an Associate Professor in the Department of Statistics, Mathematics and Informatics, Miguel Hernández University of Elche, Elche, Spain, and a Researcher in the Institute "Center of Operations Research" of the same university. His research interests are divided into two lines, namely, linear semi-infinite programming in the field of mathematics and photovoltaics in the field of engineering.

Sergio Montero was born in Beniel, Murcia, Spain, on March 24, 1987. He received the M.Sc. degree on telecommunications engineering from the University Miguel Hernández of Elche (UMH), Elche, Spain, in 2011. During his final year project he was focusing on improving the efficiency of solar power systems.

He is currently a Research Fellow at the Uwicore Laboratory, UMH, focusing on how to improve the MAC and networking operation and performance of wireless sensor networks for mobile sensing applications.

Ausiàs Garrigós (M'04) was born in Xixona, Spain, in 1976. He received the M.Sc. degree from the University of Valencia, Burjasot, Spain, in 2000, and the Ph.D. degree from the University Miguel Hernández of Elche (UMH), Elche, Spain, in 2007, both in electronics engineering.

He is currently an Associate Professor in the Department of Materials Science, Optics and Electronics Technology, UMH. His research interests include space power systems and industrial electronics.